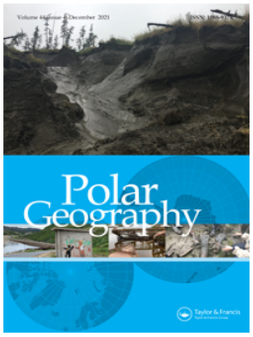

Polar Geography

ISSN: (Print) (Online) Journal homepage: https://www.tandfonline.com/loi/tpog20

A linear mixed effects model for seasonal forecasts of Arctic sea ice retreat

Sean Horvath, Julienne Stroeve & Balaji Rajagopalan

To cite this article: Sean Horvath, Julienne Stroeve & Balaji Rajagopalan (2021) A linear mixed effects model for seasonal forecasts of Arctic sea ice retreat, Polar Geography, 44:4, 297-314, DOI: 10.1080/1088937X.2021.1987999

To link to this article: https://doi.org/10.1080/1088937X.2021.1987999

Published online: 15 Oct 2021.

POLAR GEOGRAPHY
2021, VOL. 44, NO. 4, 297–314
https://doi.org/10.1080/1088937X.2021.1987999

Taylor & Francis
Taylor & Francis Group

A linear mixed effects model for seasonal forecasts of Arctic sea ice retreat

Sean Horvath [a,b], Julienne Stroeve [a,b,c] and Balaji Rajagopalan [b,d]

[a]National Snow and Ice Data Center, University of Colorado Boulder, Boulder, Colorado, USA; [b]Cooperative Institute for Research in Environmental Sciences, University of Colorado Boulder, Boulder, CO, USA; [c]Earth Sciences Department, University College of London, London, UK; [d]Department of Civil, Environmental, and Architectural Engineering, University of Colorado Boulder, Boulder, CO, USA

ABSTRACT

With sea ice cover declining in recent years, access to open Arctic waters has become a growing interest to numerous stakeholders. Access requires time for planning and preparation, which creates the need for accurate seasonal forecasts of summer sea ice characteristics. One important attribute is the timing of sea ice retreat, of which current statistical and dynamic sea ice models struggle to make accurate seasonal forecasts. We develop a linear mixed effects model to provide forecast of sea ice retreat over five major regions of the Arctic – Beaufort, Chukchi, East Siberian, Laptev, and Kara Seas. In this, the fixed effect – i.e. the mean influence of the atmosphere on sea ice retreat – is modeled using predictors that directly influence the dynamics or thermodynamics of sea ice, and random effects are grouped regionally to capture the local-scale effects on sea ice. The model exhibits very good skill in forecast of sea ice retreat at lead times of up to half a year over these regions.

ARTICLE HISTORY
Received 16 July 2020
Accepted 28 September 2021

KEYWORDS
Arctic sea ice; seasonal forecasting; statistical modeling; linear mixed effects regression; sea ice retreat

Introduction

Since satellite observations began in the late 1970s, sea ice cover in the Arctic Ocean has seen a decrease in all seasons, with an annual decrease of 4% per decade (Cavalieri & Parkinson, 2012) and the most dramatic decline experienced in September (Onarheim et al., 2018; Stroeve & Notz, 2018). Decreasing summer ice cover has led to an extension of the Arctic Ocean open water season by about a week each decade (Stroeve et al., 2014; Stroeve & Notz, 2018). This extended opening of Arctic waters has piqued interest in commercial marine transport operations (Melia et al., 2016; Stephenson et al., 2013) which require long-term planning and preparation for possible environmental disasters such as oil spills that could have consequences worse than in other ocean regions (Emmerson & Lahn, 2012). The Northern Sea Route (NSR) in particular, which would shorten travel distances by up to 40% between Asia and Europe, has received much attention (Khon et al., 2017; Stephenson et al., 2014; Yumashev et al., 2017; Zhu et al., 2018). Skillful local forecasts of sea ice attributes such as day of retreat (DOR) on seasonal time scales are therefore of great use for interested stakeholders, including industries such as marine transport, resource extraction, and tourism.

CONTACT Sean Horvath sean.horvath@colorado.edu

The changing Arctic climate and high variability of sea ice, particularly along the NSR (Figure 1), has developed interest and challenges in modeling and predicting summer sea ice conditions. Traditional forecasts focused on single value parameters such as area aggregated sea ice extent, either regionally (Drobot, 2007; Drobot & Maslanik, 2002) or pan-Arctic (Drobot et al., 2006; Lindsay et al., 2008). Recent advances in technology have made local forecasts possible that are more relevant for end users. Methods for such forecasts differ greatly but generally fall into one of two categories, (1) dynamic or numerical modeling and (2) statistical modeling. Dynamic models numerically solve systems of equations that capture the physics of sea ice using sea-ice conditions, ocean temperatures, and/or atmospheric conditions to initialize the models for each season (Msadek et al., 2014). These models can be coupled ice-ocean models with prescribed atmospheric forcing such as the Pan-Arctic Ice-Ocean Modeling Assimilation System (PIOMAS) (Zhang et al., 2008) or coupled ice-ocean-atmosphere models such as CFSv2 (Wang et al., 2012) and CanSIPS (Sigmond et al., 2013). Statistical models find relationships between sea ice and atmospheric, oceanic, or time-lagged sea ice predictors. Recently, statistical methods have been used to provide spatial field predictions of sea ice conditions using a variety of techniques such as a linear Markov model (Yuan et al., 2016), a vector autoregressive model (Wang et al., 2015), a deep neural network (Chi & Kim, 2017), and a Bayesian logistic regression (Horvath et al., 2020).

While these methods have shown promise in recent years, skillful forecasts at lead times greater than 4 months remain elusive (Bushuk et al., 2017) and accurate forecasts of extreme low or high sea ice years remains a challenge (Hamilton & Stroeve, 2016). The term 'lead time' here refers to the number of months between when a forecast is made and the time of the forecasts value (i.e. forecasting September sea ice characteristics in August is a one-month lead time). Motivated by this need, in this research we present a novel approach to seasonal forecasts of sea ice DOR by employing a linear mixed effects regression in the Beaufort, Chukchi, East Siberian, Laptev, and Kara Seas (Figure 2). Forecasts are made for one- to seven-month lead times and performance is evaluated at each pixel and aggregated by region for each lead time using a rolling-validation technique.

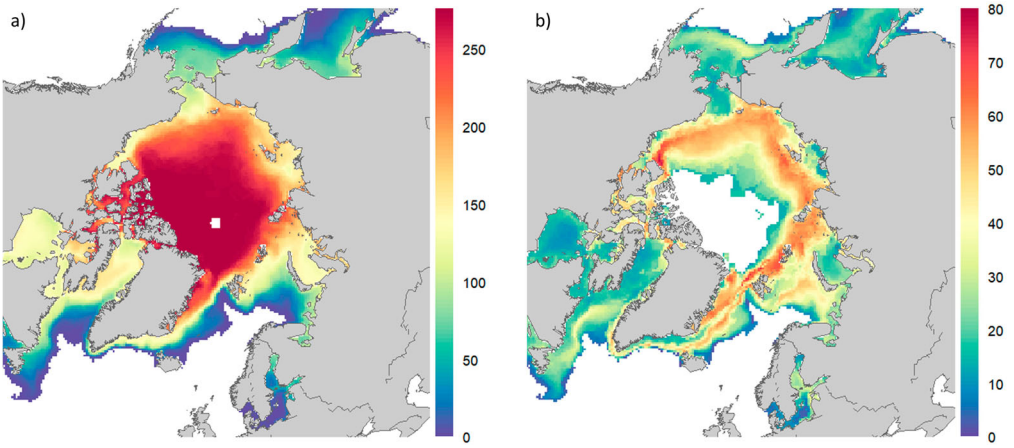

Figure 1. Aggregated sea ice statistics for years 1979–2018 showing (a) mean day of retreat and (b) standard deviation of day of retreat.

Figure 2. Subregions of the Arctic Ocean used in this study.

Data and methods

Sea ice

Sea ice concentration data is obtained from the NOAA/NSIDC Climate Data Record of Passive Microwave Sea Ice Concentration, Version 3 housed at the National Snow and Ice Data Center (NSIDC) (Meier et al., 2017). The data are derived from two sources: (1) the Near-Real-Time DMSP SSMIS Daily Polar Gridded Sea Ice Concentrations (NRTSI) from the Special Sensor Microwave Imager/Sounder (SSMIS) on board the Defense Meteorological Satellite Program (DMSP) satellites (Maslanik & Stroeve, 1999), and (2) the combined Nimbus Scanning Multichannel Microwave Radiometer (SMMR, 1979–1987), the DMSP Special Sensor Microwave/Imager (SSM/I, 1987–2007), and the Special Sensor Microwave Imager/Sounder (SSMIS, 2007 to present). Merged sea ice concentrations are used which are produced with the Climate Data Record algorithm using the NASA Team algorithm (Cavalieri et al., 1984) and the NASA Bootstrap algorithm (Comiso, 1986) covering the period from 1979 to 2018. The data is provided on a 25×25 km grid, but are aggregated to a 50×50 km grid for computational efficiency and are projected to the Equal-Area Scalable Earth Grid 2.0 (EASE-Grid 2.0) (Brodzik et al., 2012; Brodzik & Knowles, 2002). Aggregation decreases computation time but does not have a significant impact on results when compared to test runs on the native 25×25 km grid. Daily sea ice concentrations are used to produce a yearly DOR product, defined as the day of year (DOY) sea ice concentration drops below 15% and remains below 15% until autumn freeze-up (Bliss et al., 2019), where the beginning of the year is defined as March 1 (DOY 1). Following the methods of Stroeve et al. (2016), for each year at each grid cell a 5-point moving average is applied to the daily sea ice concentration time series to reduce

variability from short-term ice dynamics. Grid cells that never experience retreat are labeled *not a number* (NaN) for that year.

Sea ice motion data is obtained from the Polar Pathfinder Daily 25 km EASE-Grid Sea Ice Motion Vectors, Version 4 dataset (Tschudi et al., 2019). These motion vectors are determined by a weighted average of input sources, derived from AVHRR, AMSRE, SMMR, SSMI, and SSMI/S sensors; IABP buoys; and NCEP/NCAR Reanalysis forecasts. Daily values of eastward and northward sea ice motion are aggregated to monthly means for months January through July for years 1979 through 2018 and re-gridded to match the DOR data.

Atmospheric variables

Studies have shown that spring atmospheric conditions have a strong impact on summer sea ice melt (Kapsch et al., 2014, 2019). Building on the extensive literature studying the predictability and variability of sea ice (Huang et al., 2019; Ionita et al., 2019; Olonscheck et al., 2019; Rigor et al., 2002; Tivy et al., 2007; Wang et al., 2015, 2019; Yuan et al., 2016), local atmospheric predictors that can have a direct effect on the dynamics or thermodynamics of sea ice are used, namely downwelling longwave and shortwave radiation, and surface air temperature. All atmospheric values are derived from ERA5 (Hersbach et al., 2018). ERA5 was produced using 4D-Var data assimilation in CY41R2 of ECMWF's Integrated Forecast System (IFS), with 137 hybrid sigma/pressure (model) levels in the vertical, with the top level at 0.01 hPa. ERA5 performs very well compared to observations for downwelling shortwave and longwave radiation of the sea ice pack, although there is a positive winter bias of surface air temperature (+3.4°C) (Graham et al., 2019). Monthly mean values for months January through July for years 1979 through 2018 are projected to the EASE-Grid 2.0 and are re-gridded to match the DOR data.

Linear mixed effects model

Linear mixed effects models are an extension of linear regression models that can accommodate data collected or summarized into groups. They describe the relationship between predictor and predictand with coefficients that can vary with respect to group levels. Mixed effects models contain two parts, fixed effects terms and random effects terms where the fixed effects terms resemble traditional linear regression and the random effects terms represent variability within the group. The linear mixed effect model is defined as:

$$y = X\beta + Zb + \varepsilon \tag{1}$$

where

- y is the n-by-1 response vector, and n is the number of observations
- X is an n-by-p fixed-effects design matrix
- β is a p-by-1 fixed-effects vector
- Z is an n-by-q random-effects design matrix
- b is a q-by-1 random-effects vector, and has a prior distribution of:

$$b \sim N(0, \sigma^2 D(\theta))$$

- ε is the n-by-1 observation error vector, and has a prior distribution of:

$$\varepsilon \sim N(0, \sigma^2 I),$$

where D is a symmetric and positive semidefinite matrix, parameterized by a variance component vector θ, I is an n-by-n identity matrix, and σ^2 is the error variance.

Parameters are estimated by restricted maximum likelihood (Patterson & Thompson, 1971) which can produce unbiased estimates of variance and covariance parameters. Details of this modeling approach can be found in Bates et al. (2015). These models are widely used in social (Agasisti et al., 2017; Quené & van den Bergh, 2008; Raudenbush & Bryk, 1986; Yang & Land, 2008) and biological (Luan & Li, 2003; Tooze et al., 2010) sciences, however, our application to Arctic sea ice marks a new contribution. In this study, y is the DOR, X and Z are composed of the predictor variables described in Sections 2.1 and 2.2, and the group levels are individual pixels throughout the Arctic Ocean. In this implementation, the fixed effects represent the mean (i.e. regional) effects of the predictors, while the random effects represent small scale, more localized effects. A separate model is fit for each sea (Beaufort, Chukchi, East Siberian, Laptev, and Kara, see Figure 2) to capture regional effects, and at each lead time (5 seas × 7 lead times = 35 models). Covariate selection for each model is determined using a step-down model building approach based on the step-down strategy suggested in Zuur et al. (2009) and Diggle et al. (2002) and implemented by the 'lmerTest' package (Kuznetsova et al., 2017) in the R programming language (R Core Team, 2019). Table 1 shows the final selection of covariates for each model and is discussed further in Section 3.

Skill measurement

To test the overall performance of this model, a rolling-validation scheme is applied in which years 1980 through 1999 are used for training the model to forecast year 2000, after which years 1980 through 2000 were used to forecast year 2001, and so on through prediction year 2018. The skill is quantified via root mean squared error (RMSE) for each lead time. The MSE measures the mean squared difference between the forecasts and observations, defined as:

$$\mathrm{RMSE} = \frac{1}{N}\sum_{t=1}^{N}(f_t - o_t)^2 \tag{2}$$

where f_t are the forecasted values, o_t are the observed outcomes, and N is the number of forecasts. The RMSE takes on values in $[0,\infty)$, with a smaller score representing better predictions. To compare this technique to a reference case, the skill score (SS) is calculated by comparing the RMSE to baseline statistical models following:

$$\mathrm{SS} = 1 - \frac{\mathrm{RMSE}}{\mathrm{RMSE}^{\mathrm{ref}}} \tag{3}$$

where $RMSE^{ref}$ is the mean squared error using a baseline statistical model as the forecasted values. Here, SS=0 is when model forecasts are equal to the baseline model, SS>0 is when

Table 1. Covariates used as fixed effects and random effects for each model.

Month	Sea	Fixed effects	Random effects
January	Beaufort	conc, sat, lwdn, swdn, u, v	swdn, u
	Chukchi	conc, sat, swdn, v	lwdn, swdn, u
	East Siberian	sat, lwdn, swdn, u, v	u
	Kara	conc, sat, lwdn, swdn, u, v	1
	Laptev	conc, sat, lwdn, swdn, u, v	u
February	Beaufort	sat, lwdn, swdn, u, v	lwdn, u
	Chukchi	conc, sat, lwdn, swdn, u	u
	East Siberian	conc, sat, lwdn, swdn, u, v	u, v
	Kara	conc, sat, lwdn, swdn, u	v
	Laptev	conc, sat, lwdn, swdn, u, v	swdn
March	Beaufort	sat, lwdn, swdn, u	1
	Chukchi	conc, sat, lwdn, swdn, u, v	u, v
	East Siberian	conc, lwdn, swdn, u	swdn, u, v
	Kara	conc, sat, lwdn, swdn, u, v	lwdn, swdn, u, v
	Laptev	conc, sat, lwdn, swdn, u, v	swdn
April	Beaufort	conc, sat, lwdn, swdn, u	swdn, u
	Chukchi	conc, sat, lwdn, swdn, u, v	swdn, v
	East Siberian	conc, sat, lwdn, swdn, u, v	swdn, u, v
	Kara	conc, sat, lwdn, swdn, u, v	swdn
	Laptev	conc, lwdn, swdn, u, v	u, v
May	Beaufort	conc, sat, lwdn, swdn, u, v	swdn
	Chukchi	conc, sat, lwdn, swdn, u, v	lwdn, swdn, u, v
	East Siberian	conc, sat, lwdn, swdn, u	u, v
	Kara	conc, sat, lwdn, swdn, u, v	u
	Laptev	conc, lwdn, u	swdn, v
June	Beaufort	conc, sat, lwdn, swdn, u, v	lwdn, u, v
	Chukchi	conc, sat, lwdn, u, v	swdn, u, v
	East Siberian	conc, sat, u	u, v
	Kara	conc, lwdn, swdn, u, v	swdn, u, v
	Laptev	conc, sat, v	swdn, u, v
July	Beaufort	conc, sat, lwdn, v	lwdn
	Chukchi	conc, swdn, u, v	v
	East Siberian	conc, sat, lwdn, swdn, u, v	lwdn, u, v
	Kara	conc, sat, u	swdn, u, v
	Laptev	conc, lwdn, swdn, u, v	v

Variables are sea ice concentration (conc), surface air temperature (sat), downwelling longwave radiation (lwdn), downwelling shortwave radiation (swdn), eastward sea ice motion (u), northward sea ice motions (v), and intercept only (1).

model forecasts outperform the baseline model, and $SS<0$ is when model forecasts are worse than the baseline model. Three baseline models are used to evaluate skill score, a climatology model, a yearly persistence model, and a sea ice concentration anomaly persistence model. Climatology is calculated as the mean DOR at each grid over all the training years (e.g. when forecasting for 2015, years 1980–2014 are used to calculate the climatology). The yearly persistence model uses the previous year's DOR as the current forecast (i.e. 2017 DOR values are used as the forecast for 2018). The sea ice concentration persistence model uses sea ice concentration scaled anomalies at a given lead time to project scaled anomalies of DOR (i.e. if the sea ice concentration anomaly is one standard deviation higher than its climatological mean, then the DOR is forecasted as one standard deviation later than its climatological mean).

Results and discussion

Covariate selection

The final selection of covariates for each model shows a range of configurations with no common covariate used in every model. However, in general, the models using January

through May predictors use most of the covariates as fixed effects while June and July models use a smaller subset. For all of the models, only radiation and sea ice motion vectors are ever used as random effects. In general, sea ice concentrations and surface air temperatures exhibit a spatial pattern similar to the DOR response variable while the radiation and sea ice motion variables do not (not shown). Hence, coefficients for radiation and sea ice motion covariates vary spatially for many model selections. Figure 3 shows the coefficients of the three covariates in the random effect over the Arctic seas at three lead times – the spatial and temporal variability is quite apparent. However, the coefficients vary rather smoothly in space which is not a priori included in the model. Interestingly, the combination of fixed and random effects seems to allow the model to capture the spatial coherence among the regression coefficients (Figure 3).

An unexpected outcome of this covariate selection method is that downwelling shortwave radiation is included in models fitted using winter predictors despite a lack of

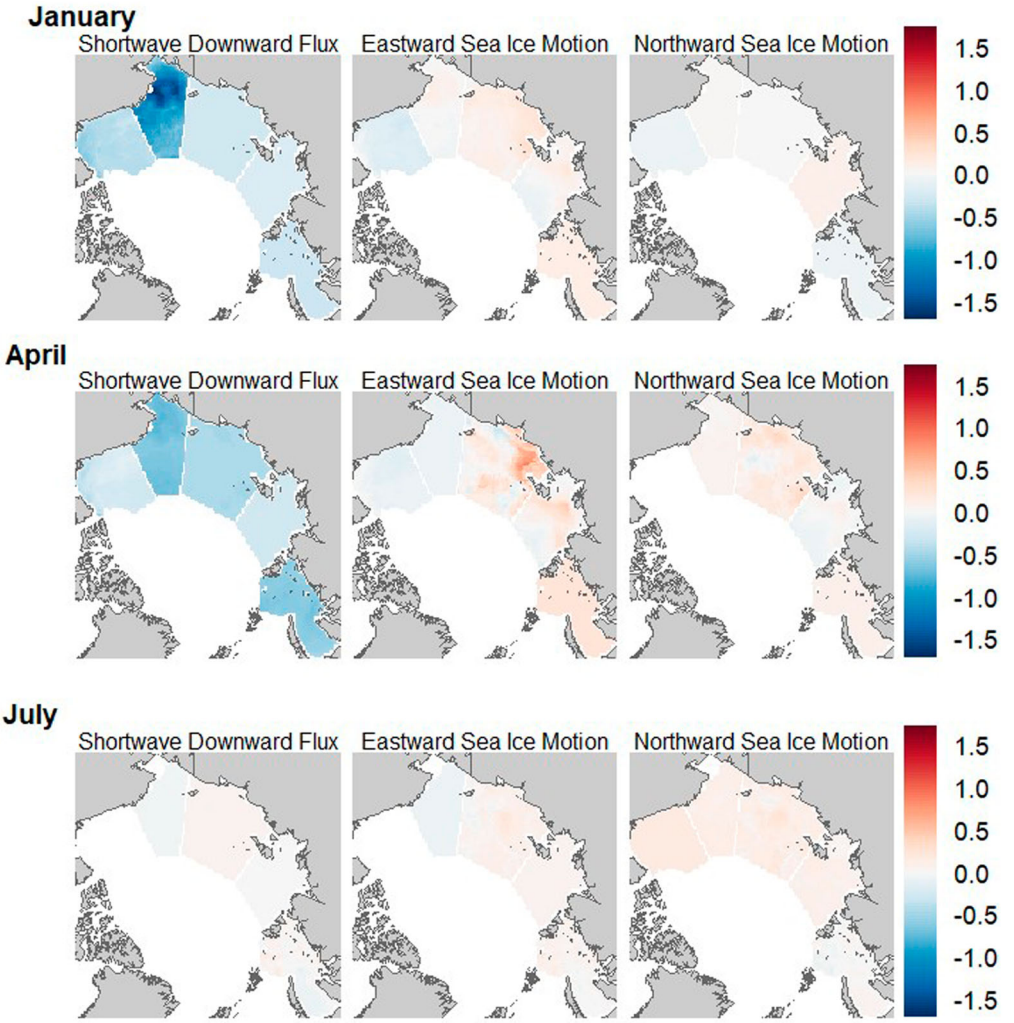

Figure 3. Regression coefficients for shortwave downward flux and vector components of sea ice motion. Values are shown for 1-, 4-, and 7-month lead times.

incoming shortwave radiation during Arctic winters. However, in the southern portion of each of these seas, there is a small shortwave signal. Because the shortwave covariate is zero at most grid cells, inclusion of this regression coefficient does not degrade performance at these grid cells and is able to add skill to forecasts made in the southern regions.

Model skill

Model skill is determined by RMSE calculated separately at each grid cell for each model and lead time, shown in Figure 4(a). In general, higher skill (i.e. lower RMSE) is demonstrated near the sea ice edge and near coastal locations, with slightly worse skill in the marginal ice zone. Skill in the marginal ice zone however does increase as lead time decreases. Two regions with less skill are apparent, especially at longer lead times, namely near the

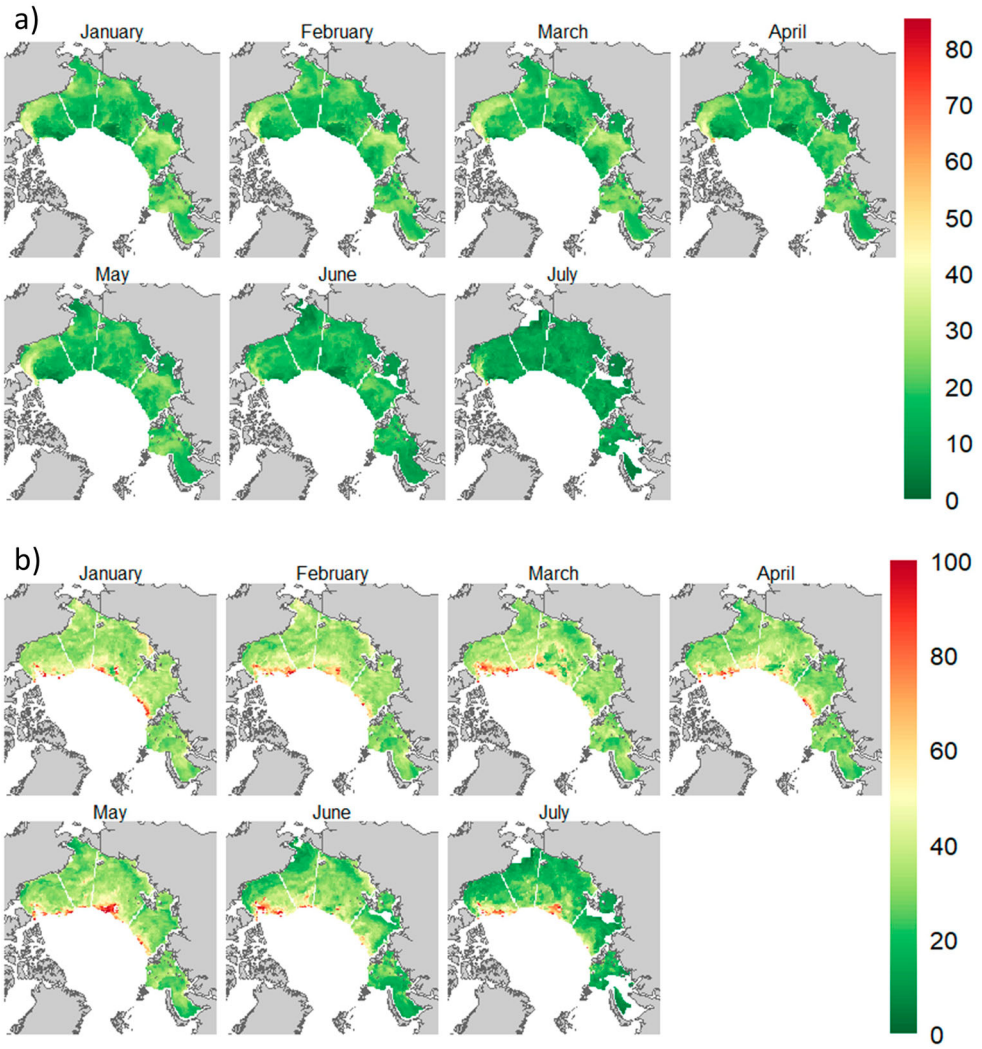

Figure 4. Skill scores plotted for each lead time (January through July). Skill scores shown are (a) RMSE, and (b) RMSE as a percentage of the range of observed values at each location.

coast in the eastern Beaufort Sea and in the mid-latitude Laptev Sea, two areas with high DOR variability (Figure 1(b)).

Because the variability differs at each location, we computed the RMSE as a percentage of the range of observed values at each grid cell (Figure 4(b)). Areas at high latitudes near the more permanent ice edge show RMSE scores that approach the range of observed values, while lower latitudes show a reduction in RMSE percentages. Higher RMSE percentage values at high latitudes are due to a smaller range of observed values. The areas with high RMSE scores in the eastern Beaufort Sea and in the mid-latitude Laptev Sea show lower RMSE percentages due to a wider range of observed values. The latitudinal variation in RMSE percentages seen in Figure 4(a), particularly in June and July, could also be a result of earlier retreat at southern locations. Forecasts of July DOR made using June predictors, for example, are actually a sub-monthly lead time and so can inflate the forecast skill.

Forecast skill scores through rolling validation

The rolling-validation skill scores (found individually at each grid cell) comparing our model to three baseline statistical models show high forecast skill across most of the domain at all lead times, especially at higher latitudes (Figure 5). As lead time decreases, skill improves compared to climatology. We recognize that the atmospheric circulation variables and the sea ice attributes exhibit a strong trend over the study period. To compare the performance of our model against this, we computed skills relative to a linear trend model, shown in Figure 5(b). The difference in skill between long lead times and short lead times is more apparent using the linear trend model. Using January through May predictors, the linear trend outperforms our model in most of the Chukchi Sea and the southern Beaufort Sea, as well as along the Siberian coastline.

We also compared the skill of our model against an anomaly persistence model in which the scaled sea ice concentration anomaly is assumed to be the scaled DOR anomaly. Skill tends to decrease slightly as lead time decreases compared to the sea ice concentration persistence model (Figure 5(c)). This is likely due to stronger predictive power from sea ice concentration as the summer progresses. Similarly, higher skill at long lead times compared to the sea ice concentration persistence model can be explained by lower variability in sea ice concentration during the winter and spring as well as spring atmospheric conditions affecting melt onset which impacts ice retreat later in the season (e.g. Stroeve et al., 2016).

By observing the regression coefficients for each region and at each lead time we can better understand what the sources of predictability are. Shortwave and longwave radiation are important predictors for most regions using January through April predictors. Shortwave radiation typically has a larger regression coefficient until April when the regression coefficient for longwave radiation becomes greater in the Kara, Laptev, and East Siberian seas. By the summer months (June and July), sea ice concentration is the most influential predictor.

The magnitude of regression coefficients using May predictors are more evenly distributed than any other month. Shortwave and longwave radiation remain important predictors for most regions along with sea ice concentration. The importance of other predictors varies by region. For instance, the regression coefficient for the v-component of sea ice motion is large in the Chukchi sea, while the regression coefficient for the u-component of sea ice motion is large in the Beaufort Sea. This shift of variable importance from atmospheric predictors to sea ice predictors from April to June suggest that May is a

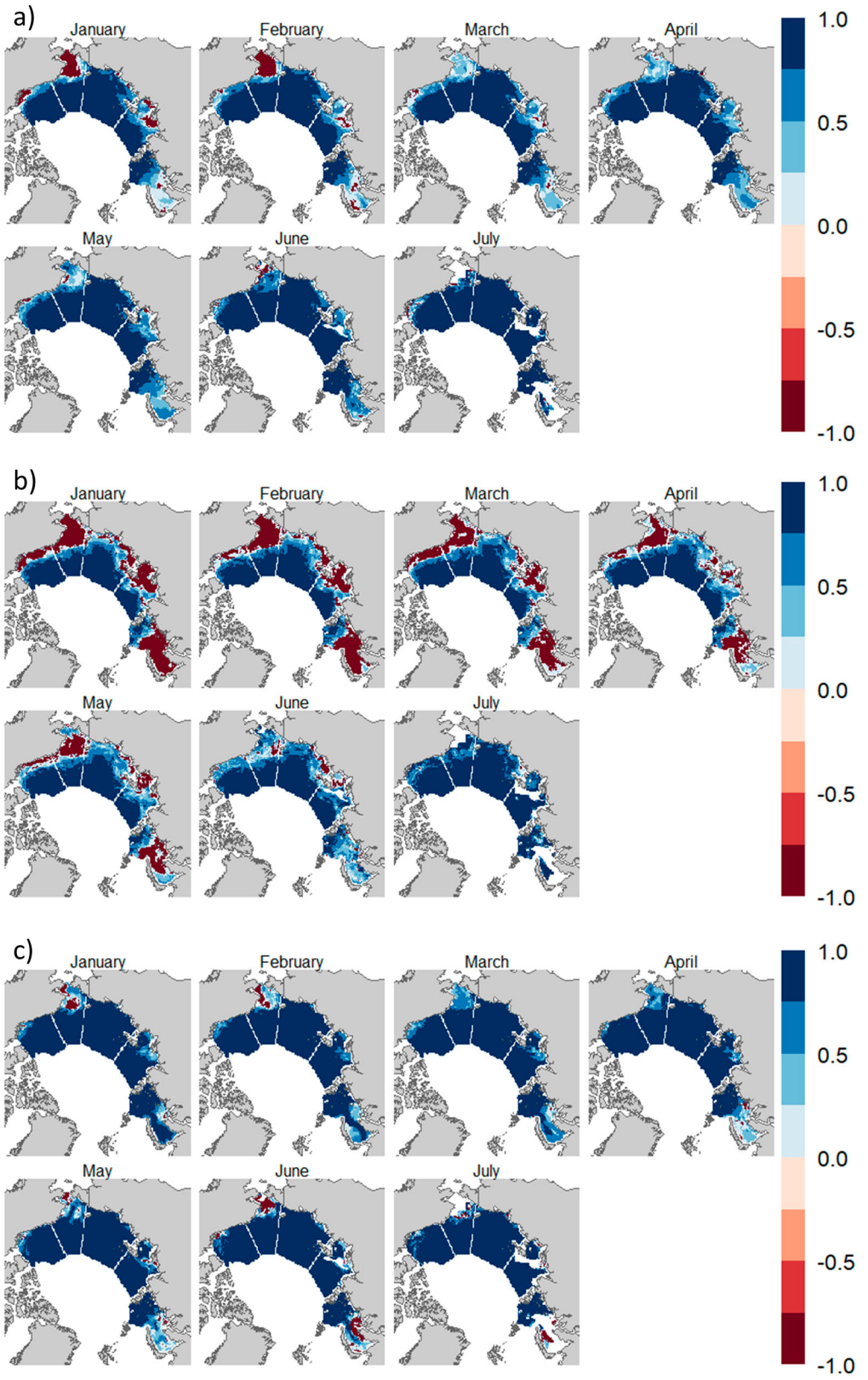

Figure 5. Spatial maps of the rolling-validation skill scores at all lead times compared to (a) climatology, (b) yearly persistence, and (c) sea ice concentration persistence. Positive skill scores mean the forecast out-performs the baseline model.

transition period in the Arctic. This is reminiscent of perfect model experiments that found a large decrease in prediction skill when dynamical models are initialized prior to June 1st (Bonan et al., 2019; Bushuk et al., 2018, 2020; Day et al., 2014). This may also explain why the linear trend is better than the forecast model in some areas prior to June.

Areas in the southern Chukchi sea show less skill compared to all three baseline models than elsewhere in the Arctic. This area is exposed to incoming oceanic heat from the Pacific Ocean through the Bering Strait. Maximum heat inflow typically occurs in August and September but can happen as early as June or as late as October (Serreze et al., 2016). This shallowness of the Bering Strait results in a near-surface heat source that has been linked to seasonal retreat of the ice pack in the Chukchi Sea (Ahlnäs & Garrison, 1984; Fedorova & Yankina, 1964; Paquette & Bourke, 1974; Serreze et al., 2016; Spall, 2007; Woodgate et al., 2010, 2015). Serreze et al. (2016) found a strong correlation (−0.80) between heat influx through the Bering Strait (April through June) and sea ice retreat date in the Chukchi Sea. They also showed that the Bering Strait heat influx accounts for about two thirds of the variance in retreat day (detrended). Oceanic heat flux data is collected from a system of moorings in the Bering Strait as part of the NSF-Arctic Observing Network program (Woodgate et al., 2015).

Two other areas demonstrate noticeably lower skill, the southern Laptev Sea and the southern Kara Sea, both of which contain large quantities of river discharge during spring and summer. While most of the Laptev Sea has been found to be largely unaffected by river discharge, sea ice coverage in the eastern Laptev Sea is influenced by Lena river discharge (Bareiss et al., 1999). Additional studies have shown that ice cover in the Laptev Sea is largely driven by atmospheric forcing (Alexandrov et al., 2000) but that local melting near coastal outlets is tied to river water (Bareiss & Görgen, 2005; Bauch et al., 2013). Lena River runoff may contribute to sea ice retreat via increased solar radiation absorption by suspended particulate matter and colored dissolved organic matter within the river discharge (Granskog et al., 2007; Hill, 2008). In early spring, river water may flood the ice covered Lena River delta directly facilitating sea ice melt (Bareiss et al., 1999). This river water may pool near the Lena River outflow before being dispersed north or eastward by prevailing winds (Bauch et al., 2013).

Studies of the predictability of sea ice retreat specific to the Kara Sea are far less prevalent in the literature. However, the Kara Sea does have an inflow of warmer oceanic water from the Atlantic via the Barents Sea and the Kara Strait (Harms & Karcher, 1999; Pfirman et al., 1997) as well as substantial river discharge from the Ob and Yenisei rivers (Pavlov & Pfirman, 1995). These mechanisms may drive sea ice retreat similar to the Chukchi and Laptev Seas.

A yearly RMSE score per sea is calculated by aggregating all DOR forecasts made for a given year by region and comparing them to observed values (Figure 6(a)). RMSE scores remain fairly constant in the range of 15–25 days at lead times between 3- and 7-months, but there is a noticeable improvement in skill scores as lead time decreases to 2- and 1-month. Values in the Beaufort and Laptev Seas are noticeably larger at long lead times compared to the remaining regions, similar to the scores calculated in Figure 4.

Biases in forecasts can be determined by examining the average difference between forecasts and observations aggregated by lead time for each region (Figure 6(b)). The Chukchi, Kara, and to a lesser degree Laptev Seas show bias forecasting DOR later than observed most years. This is likely due to oceanic heat influxes and the influence of river runoff discussed previously that are not included as predictors in this study. The less severe bias in the

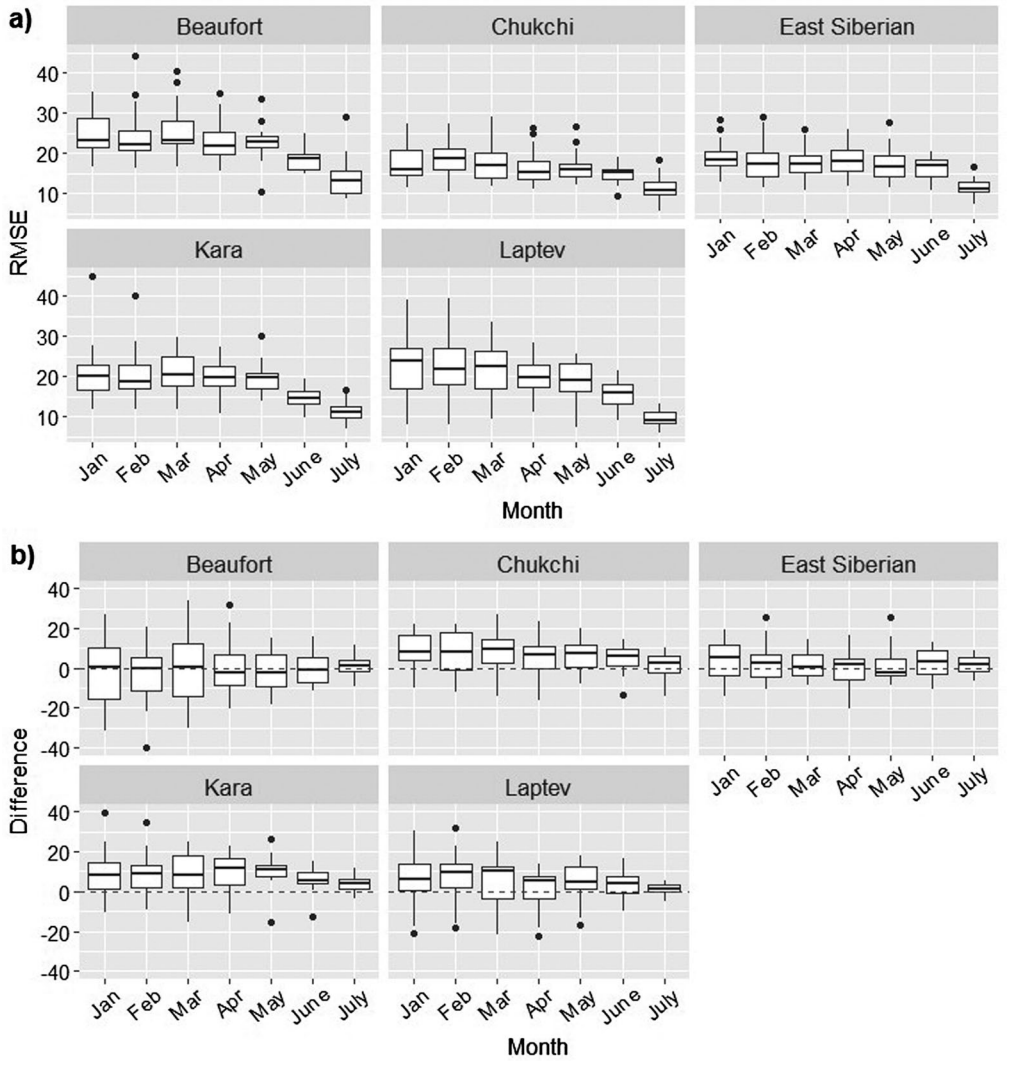

Figure 6. Yearly averaged (a) RMSE and (b) difference between forecasted and observed values grouped by region and lead time.

Laptev Sea suggests that oceanic heat influx has a stronger influence on sea ice retreat than river runoff.

Summary and conclusion

With the projected continual expansion of open ocean conditions in the Arctic comes the need for skillful seasonal forecasts. This study presents a linear mixed effects regression model for forecasts of the day of sea ice retreat. Individual models are developed for five Arctic regions (Beaufort, Chukchi, East Siberian, Laptev, and Kara Seas) at lead times of one- to seven-months. Sea ice concentration, surface air temperature, longwave and shortwave downwelling radiation, and vector components of sea ice motion are used as predictors and model selection via a step-down approach further reduces the chosen predictors.

The random effect is grouped by grid cell, allowing the model to capture local-scale variability while the fixed effect captures mean effects. Forecasts in all regions and at all lead times are shown to be skillful compared to three baseline statistical models; climatology, yearly persistence, and sea ice concentration anomaly persistence. Stakeholders interested in accurate forecasts of sea ice retreat could rely on this method for 3–7 month lead times with an accuracy of about 20 days, a 2 month lead time with an accuracy of about 15 days, and a 1 month lead time with an accuracy of about 10 days.

There is potential to improve this model's performance. Consideration of more covariates could provide additional skill, especially at longer lead times. Factors known to contribute to sea ice conditions, such as oceanic heat fluxes and river runoff, could assuage forecast errors in the Chukchi, Laptev, and Kara Seas. Sea ice thickness, particularly after melt onset has occurred, has been identified as an important predictor of summer sea ice (Bushuk et al., 2020). Climate indices could provide useful information about the large scale state of the atmosphere and ocean. A spatial component could be used in lieu of random effects to capture the spatial variability efficiently (Cressie & Wikle, 2015). Also a Bayesian Hierarchical framework can be used to quantify the uncertainties robustly (Clark & Gelfand, 2006). This method could also be expanded upon to include the forecast of additional sea ice attributes of interest such as day of advance (and therefore length of the open water season). Furthermore, forecasts from various models (dynamical and statistical) including this one can be combined robustly (Krishnamurti et al., 1999) to provide multi-model probabilistic forecast that will further enhance the skill. Our novel modeling approach opens encouraging prospects for skillful seasonal forecasts of sea ice attributes that are crucial to enable safer, more sustainable, and socioeconomically beneficial access to the Arctic Ocean.

Acknowledgements

We acknowledge the contributions of the late Drew Slater. All data used is publicly available from ECMWF (https://www.ecmwf.int/en/forecasts/datasets/reanalysis-datasets/era5) and NSIDC (https://nsidc.org/data).

Disclosure statement

No potential conflict of interest was reported by the author(s).

Funding

This work was supported by National Oceanic and Atmospheric Administration [grant number: NA15OAR4310171].

ORCID

Sean Horvath http://orcid.org/0000-0002-6462-0722
Julienne Stroeve http://orcid.org/0000-0001-7316-8320
Balaji Rajagopalan http://orcid.org/0000-0002-6883-7240

References

Agasisti, T., Ieva, F., & Paganoni, A. M. (2017). Heterogeneity, school-effects and the north/south achievement gap in Italian secondary education: Evidence from a three-level mixed model. *Statistical Methods & Applications*, *26*(1), 157–180. https://doi.org/10.1007/s10260-016-0363-x

Ahlnäs, K., & Garrison, G. R. (1984). Satellite and oceanographic observations of the warm coastal current in the Chukchi Sea. *Arctic*, *37*(3), 244–254. https://doi.org/10.14430/arctic2197

Alexandrov, V. Y., Martin, T., Kolatschek, J., Eicken, H., Kreyscher, M., & Makshtas, A. P. (2000). Sea ice circulation in the Laptev Sea and ice export to the Arctic Ocean: Sea ice circulation in the Laptev Sea and ice export to the Arctic Ocean: Results from satellite remote sensing and numerical modeling. *Journal of Geophysical Research: Oceans*, *105*(C7), 17143–17159. https://doi.org/10.1029/2000JC900029

Bareiss, J., Eicken, H., Helbig, A., & Martin, T. (1999). Impact of river discharge and regional climatology on the decay of Sea Ice in the Laptev Sea during spring and early summer. *Arctic, Antarctic, and Alpine Research*, *31*(3), 214–229. https://doi.org/10.1080/15230430.1999.12003302

Bareiss, J., & Görgen, K. (2005). Spatial and temporal variability of sea ice in the Laptev Sea: Analyses and review of satellite passive-microwave data and model results, 1979 to 2002. *Global and Planetary Change*, *48*(1), 28–54. https://doi.org/10.1016/j.gloplacha.2004.12.004

Bates, D., Mächler, M., Bolker, B., & Walker, S. (2015). Fitting linear mixed-effects models using lme4. *Journal of Statistical Software*, *67*(1), 1–48. https://doi.org/10.18637/jss.v067.i01

Bauch, D., Hölemann, J. A., Nikulina, A., Wegner, C., Janout, M. A., Timokhov, L. A., & Kassens, H. (2013). Correlation of river water and local sea-ice melting on the Laptev Sea shelf (Siberian Arctic). *Journal of Geophysical Research: Oceans*, *118*(1), 550–561. https://doi.org/10.1002/jgrc.20076

Bliss, A. C., Steele, M., Peng, G., Meier, W. N., & Dickinson, S. (2019). Regional variability of Arctic sea ice seasonal change climate indicators from a passive microwave climate data record. *Environmental Research Letters*, *14*(4), 045003. https://doi.org/10.1088/1748-9326/aafb84

Bonan, D. B., Bushuk, M., & Winton, M. (2019). A spring barrier for regional predictions of summer Arctic Sea Ice. *Geophysical Research Letters*, *46*(11), 5937–5947. https://doi.org/10.1029/2019GL082947

Brodzik, M. J., Billingsley, B., Haran, T., Raup, B., & Savoie, M. (2012). EASE-Grid 2.0: Incremental but significant improvements for earth-gridded data sets. *ISPRS International Journal of Geo-Information*, *1*(1), 32–45. https://doi.org/10.3390/ijgi1010032

Brodzik, M. J., & Knowles, K. W. (2002). Chapter 5: EASE-grid: A versatile Set of Equal-Area projections and grids. In M. Goodchild (Ed.), *Discrete Global Grids* (pp. 98–113). Santa Barbara, CA: National Center for Geographic Information & Analysis. https://escholarship.org/uc/item/9492q6sm

Bushuk, M., Msadek, R., Winton, M., Vecchi, G. A., Gudgel, R., Rosati, A., & Yang, X. (2017). Skillful regional prediction of Arctic sea ice on seasonal timescales. *Geophysical Research Letters*, *44*(10), 4953–4964. https://doi.org/10.1002/2017GL073155

Bushuk, M., Msadek, R., Winton, M., Vecchi, G., Yang, X., Rosati, A., & Gudgel, R. (2018). Regional Arctic sea–ice prediction: Potential versus operational seasonal forecast skill. *Climate Dynamics*, *52*(5), 2721–2743. https://doi.org/10.1007/s00382-018-4288-y

Bushuk, M., Winton, M., Bonan, D. B., Blanchard-Wrigglesworth, E., & Delworth, T. L. (2020). A mechanism for the Arctic Sea Ice spring predictability barrier. *Geophysical Research Letters*, *47*(13), Article e2020GL088335. https://doi.org/10.1029/2020GL088335

Cavalieri, D. J., Gloersen, P., & Campbell, W. J. (1984). Determination of sea ice parameters with the NIMBUS 7 SMMR. *Journal of Geophysical Research: Atmospheres*, *89*(D4), 5355–5369. https://doi.org/10.1029/JD089iD04p05355

Cavalieri, D. J., & Parkinson, C. L. (2012). Arctic sea ice variability and trends, 1979–2010. *The Cryosphere*, *6*(4), 881–889. https://doi.org/10.5194/tc-6-881-2012

Chi, J., & Kim, H. (2017). Prediction of Arctic Sea Ice concentration using a fully data driven deep neural network. *Remote Sensing*, *9*(12), 1305. https://doi.org/10.3390/rs9121305

Clark, J. S., & Gelfand, A. E. (2006). *Hierarchical modelling for the environmental sciences: Statistical methods and applications*. Oxford University Press.

Comiso, J. C. (1986). Characteristics of Arctic winter sea ice from satellite multispectral microwave observations. *Journal of Geophysical Research: Oceans*, *91*(C1), 975–994. https://doi.org/10.1029/JC091iC01p00975

Cressie, N., & Wikle, C. K. (2015). *Statistics for spatio-temporal data*. John Wiley & Sons.

Day, J. J., Tietsche, S., & Hawkins, E. (2014). Pan-Arctic and regional Sea Ice predictability: Initialization month dependence. *Journal of Climate*, *27*(12), 4371–4390. https://doi.org/10.1175/JCLI-D-13-00614.1

Diggle, P., Heagerty, P., Liang, K.-Y., Heagerty, P. J., & Zeger, S. (2002). *Analysis of longitudinal data*. OUP.

Drobot, S. D. (2007). Using remote sensing data to develop seasonal outlooks for Arctic regional sea-ice minimum extent. *Remote Sensing of Environment*, *111*(2), 136–147. https://doi.org/10.1016/j.rse.2007.03.024

Drobot, S. D., & Maslanik, J. A. (2002). A practical method for long-range forecasting of ice severity in the Beaufort Sea. *Geophysical Research Letters*, *29*(8), 54-1–54-4. https://doi.org/10.1029/2001GL014173

Drobot, S. D., Maslanik, J. A., & Fowler, C. (2006). A long-range forecast of Arctic summer sea-ice minimum extent. *Geophysical Research Letters*, *33*(10), L10501. https://doi.org/10.1029/2006GL026216

Emmerson, C., & Lahn, G. (2012, May 30). *Arctic opening: Opportunity and risk in the high north* [Monograph]. Chatham House. http://library.arcticportal.org/1671/.

Fedorova, Z. P., & Yankina, Z. S. (1964). The passage of Pacific Ocean water through the Bering Strait into the Chukchi Sea. *Deep Sea Research and Oceanographic Abstracts*, *11*(3), 423–425. https://doi.org/10.1016/0011-7471(64)90539-X

Graham, R. M., Cohen, L., Ritzhaupt, N., Segger, B., Graversen, R. G., Rinke, A., Walden, V. P., Granskog, M. A., & Hudson, S. R. (2019). Evaluation of six atmospheric reanalyses over Arctic sea ice from winter to early summer. *Journal of Climate*, *32*(14), 4121–4143. https://doi.org/10.1175/JCLI-D-18-0643.1

Granskog, M. A., Macdonald, R. W., Mundy, C.-J., & Barber, D. G. (2007). Distribution, characteristics and potential impacts of chromophoric dissolved organic matter (CDOM) in Hudson Strait and Hudson Bay, Canada. *Continental Shelf Research*, *27*(15), 2032–2050. https://doi.org/10.1016/j.csr.2007.05.001

Hamilton, L. C., & Stroeve, J. (2016). 400 predictions: The SEARCH Sea Ice outlook 2008–2015. *Polar Geography*, *39*(4), 274–287. https://doi.org/10.1080/1088937X.2016.1234518

Harms, I. H., & Karcher, M. J. (1999). Modeling the seasonal variability of hydrography and circulation in the Kara Sea. *Journal of Geophysical Research: Oceans*, *104*(C6), 13431–13448. https://doi.org/10.1029/1999JC900048

Hersbach, H., Bell, B., Berrisford, P., Biavati, G., Horányi, A., Muñoz Sabater, J., Nicolas, J., Peubey, C., Radu, R., Rozum, I., Schepers, D., Simmons, A., Soci, C., Dee, D., & Thépaut, J.-N. (2018). ERA5 hourly data on pressure levels from 1979 to present. Copernicus Climate Change Service (C3S) Climate Data Store (CDS). https://doi.org/10.24381/cds.bd0915c6

Hill, V. J. (2008). Impacts of chromophoric dissolved organic material on surface ocean heating in the Chukchi Sea. *Journal of Geophysical Research: Oceans*, *113*(C7), C07024. https://doi.org/10.1029/2007JC004119

Horvath, S., Stroeve, J., Rajagopalan, B., & Kleiber, W. (2020). A Bayesian logistic regression for probabilistic forecasts of the minimum September Arctic Sea Ice cover. *Earth and Space Science*, *7*(10), e2020EA001176. https://doi.org/10.1029/2020EA001176

Huang, Y., Dong, X., Bailey, D. A., Holland, M. M., Xi, B., DuVivier, A. K., Kay, J. E., Landrum, L. L., & Deng, Y. (2019). Thicker clouds and accelerated Arctic Sea Ice decline: The atmosphere-Sea Ice interactions in spring. *Geophysical Research Letters*, *46*(12), 6980–6989. https://doi.org/10.1029/2019GL082791

Ionita, M., Grosfeld, K., Scholz, P., Treffeisen, R., & Lohmann, G. (2019). September Arctic sea ice minimum prediction – a skillful new statistical approach. *Earth System Dynamics*, *10*(1), 189–203. https://doi.org/10.5194/esd-10-189-2019

Kapsch, M.-L., Graversen, R. G., Economou, T., & Tjernström, M. (2014). The importance of spring atmospheric conditions for predictions of the Arctic summer sea ice extent. *Geophysical Research Letters*, *41*(14), 5288–5296. https://doi.org/10.1002/2014GL060826

Kapsch, M.-L., Skific, N., Graversen, R. G., Tjernström, M., & Francis, J. A. (2019). Summers with low Arctic sea ice linked to persistence of spring atmospheric circulation patterns. *Climate Dynamics*, *52*(3), 2497–2512. https://doi.org/10.1007/s00382-018-4279-z

Khon, V. C., Mokhov, I. I., & Semenov, V. A. (2017). Transit navigation through Northern Sea Route from satellite data and CMIP5 simulations. *Environmental Research Letters*, *12*(2), 024010. https://doi.org/10.1088/1748-9326/aa5841

Krishnamurti, T. N., Kishtawal, C. M., LaRow, T. E., Bachiochi, D. R., Zhang, Z., Williford, C. E., Gadgil, S., & Surendran, S. (1999). Improved Weather and seasonal Climate forecasts from multimodel superensemble. *Science*, *285*(5433), 1548–1550. https://doi.org/10.1126/science.285.5433.1548

Kuznetsova, A., Brockhoff, P. B., & Christensen, R. H. B. (2017). Lmertest package: Tests in linear mixed effects models. *Journal of Statistical Software*, *82*(1), 1–26. https://doi.org/10.18637/jss.v082.i13

Lindsay, R. W., Zhang, J., Schweiger, A. J., & Steele, M. A. (2008). Seasonal predictions of ice extent in the Arctic ocean. *Journal of Geophysical Research: Oceans*, *113*(C2), C02023. https://doi.org/10.1029/2007JC004259

Luan, Y., & Li, H. (2003). Clustering of time-course gene expression data using a mixed-effects model with B-splines. *Bioinformatics*, *19*(4), 474–482. https://doi.org/10.1093/bioinformatics/btg014

Maslanik, J., & Stroeve, J. (1999). Near-real-time DMSP SSM/I-SSMIS daily polar gridded sea ice concentrations, Version 1. NASA National Snow and Ice Data Center Distributed Active Archive Center. https://doi.org/10.5067/U8C09DWVX9LM

Meier, W. N., Fetterer, F., Savoie, M., Mallory, S., Duerr, R., & Stroeve, J. (2017). *NOAA/NSIDC climate data record of passive microwave sea ice concentration* (Version 3). Merged GSFC NASA Team/Bootstrap daily sea ice concentrations. NSIDC: National Snow and Ice Data Center. https://doi.org/10.7265/N59P2ZTG.

Melia, N., Haines, K., & Hawkins, E. (2016). Sea ice decline and 21st century trans-Arctic shipping routes. *Geophysical Research Letters*, *43*(18), 9720–9728. https://doi.org/10.1002/2016GL069315

Msadek, R., Vecchi, G. A., Winton, M., & Gudgel, R. G. (2014). Importance of initial conditions in seasonal predictions of Arctic sea ice extent. *Geophysical Research Letters*, *41*(14), 5208–5215. https://doi.org/10.1002/2014GL060799

Olonscheck, D., Mauritsen, T., & Notz, D. (2019). Arctic sea-ice variability is primarily driven by atmospheric temperature fluctuations. *Nature Geoscience*, *12*(6), 430–434. https://doi.org/10.1038/s41561-019-0363-1

Onarheim, I. H., Eldevik, T., Smedsrud, L. H., & Stroeve, J. C. (2018). Seasonal and regional manifestation of Arctic Sea Ice loss. *Journal of Climate*, *31*(12), 4917–4932. https://doi.org/10.1175/JCLI-D-17-0427.1

Paquette, R. G., & Bourke, R. H. (1974). Observations on the coastal current of Arctic Alaska. *J. Mar. Res.*, *32*, 195–207. https://doi.org/10.1016/j.dsr2.2005.10.015

Patterson, H. D., & Thompson, R. (1971). Recovery of inter-block information when block sizes are unequal. *Biometrika*, *58*(3), 545–554. https://doi.org/10.1093/biomet/58.3.545

Pavlov, V. K., & Pfirman, S. L. (1995). Hydrographic structure and variability of the Kara Sea: Implications for pollutant distribution. *Deep Sea Research Part II: Topical Studies in Oceanography*, *42*(6), 1369–1390. https://doi.org/10.1016/0967-0645(95)00046-1

Pfirman, S. L., Kögeler, J. W., & Rigor, I. (1997). Potential for rapid transport of contaminants from the Kara Sea. *Science of The Total Environment*, *202*(1), 111–122. https://doi.org/10.1016/S0048-9697(97)00108-3

Quené, H., & van den Bergh, H. (2008). Examples of mixed-effects modeling with crossed random effects and with binomial data. *Journal of Memory and Language*, *59*(4), 413–425. https://doi.org/10.1016/j.jml.2008.02.002

R Core Team. (2019). *R: A language and environment for statistical computing*. R Foundation for Statistical Computing. https://www.R-project.org/.

Raudenbush, S., & Bryk, A. S. (1986). A Hierarchical Model for studying school effects. *Sociology of Education*, *59*(1), 1–17. https://doi.org/10.2307/2112482

Rigor, I. G., Wallace, J. M., & Colony, R. L. (2002). Response of Sea Ice to the Arctic oscillation. *Journal of Climate*, *15*(18), 2648–2663. https://doi.org/10.1175/1520-0442(2002)015<2648:ROSITT>2.0.CO;2

Serreze, M. C., Crawford, A. D., Stroeve, J. C., Barrett, A. P., & Woodgate, R. A. (2016). Variability, trends, and predictability of seasonal sea ice retreat and advance in the Chukchi Sea. *Journal of Geophysical Research: Oceans*, *121*(10), 7308–7325. https://doi.org/10.1002/2016JC011977

Sigmond, M., Fyfe, J. C., Flato, G. M., Kharin, V. V., & Merryfield, W. J. (2013). Seasonal forecast skill of Arctic sea ice area in a dynamical forecast system. *Geophysical Research Letters*, *40*(3), 529–534. https://doi.org/10.1002/grl.50129

Spall, M. A. (2007). Circulation and water mass transformation in a model of the Chukchi Sea. *Journal of Geophysical Research*, *112*, C05025. https://doi.org/10.1029/2005JC003364

Stephenson, S. R., Brigham, L. W., & Smith, L. C. (2014). Marine accessibility along russia's Northern Sea route. *Polar Geography*, *37*(2), 111–133. https://doi.org/10.1080/1088937X.2013.845859

Stephenson, S. R., Smith, L. C., Brigham, L. W., & Agnew, J. A. (2013). Projected 21st-century changes to Arctic marine access. *Climatic Change*, *118*(3), 885–899. https://doi.org/10.1007/s10584-012-0685-0

Stroeve, J. C., Crawford, A. D., & Stammerjohn, S. (2016). Using timing of ice retreat to predict timing of fall freeze-up in the Arctic. *Geophysical Research Letters*, *43*(12), 6332–6340. https://doi.org/10.1002/2016GL069314

Stroeve, J., Markus, T., Boisvert, L., Miller, J., & Barrett, A. (2014). Changes in Arctic melt season and implications for sea ice loss. *Geophysical Research Letters*, *41*(4), 1216–1225. https://doi.org/10.1002/2013GL058951

Stroeve, J., & Notz, D. (2018). Changing state of Arctic sea ice across all seasons. *Environmental Research Letters*, *13*(10), 103001. https://doi.org/10.1088/1748-9326/aade56

Tivy, A., Alt, B., Howell, S., Wilson, K., & Yackel, J. (2007). Long-range prediction of the shipping season in Hudson Bay: A statistical approach. *Weather and Forecasting*, *22*(5), 1063–1075. https://doi.org/10.1175/WAF1038.1

Tooze, J. A., Kipnis, V., Buckman, D. W., Carroll, R. J., Freedman, L. S., Guenther, P. M., Krebs-Smith, S. M., Subar, A. F., & Dodd, K. W. (2010). A mixed-effects model approach for estimating the distribution of usual intake of nutrients: The NCI method. *Statistics in Medicine*, *29*(27), 2857–2868. https://doi.org/10.1002/sim.4063

Tschudi, M., Meier, W. N., Stewart, J. S., Fowler, C., & Maslanik, J. (2019). *Polar pathfinder daily 25km EASE-grid sea ice motion vectors* (Version 4). NASA National Snow and Ice Data Center Distributed Active Archive Center. https://doi.org/10.5067/INAWUWO7QH7B.

Wang, L., Yuan, X., & Li, C. (2019). Subseasonal forecast of Arctic sea ice concentration via statistical approaches. *Climate Dynamics*, *52*(7), 4953–4971. https://doi.org/10.1007/s00382-018-4426-6

Wang, L., Yuan, X., Ting, M., & Li, C. (2015). Predicting summer Arctic Sea Ice concentration intra-seasonal variability using a vector autoregressive model. *Journal of Climate*, *29*(4), 1529–1543. https://doi.org/10.1175/JCLI-D-15-0313.1

Wang, W., Chen, M., & Kumar, A. (2012). Seasonal prediction of Arctic Sea Ice extent from a coupled dynamical forecast system. *Monthly Weather Review*, *141*(4), 1375–1394. https://doi.org/10.1175/MWR-D-12-00057.1

Woodgate, R. A., Stafford, K. M., & Prahl, F. G. (2015). A synthesis of year-round interdisciplinary mooring measurements in the Bering Strait (1990–2014) and the RUSALCA years (2004–2011). *Oceanography*, *28*(3), 46–67. https://doi.org/10.5670/oceanog.2015.57

Woodgate, R. A., Weingartner, T., & Lindsay, R. (2010). The 2007 Bering Strait oceanic heat flux and anomalous Arctic sea-ice retreat. *Geophysical Research Letters*, *37*(1), L01602. https://doi.org/10.1029/2009GL041621

Yang, Y., & Land, K. C. (2008). Age–period–cohort Analysis of repeated cross-Section surveys: Fixed or random effects? *Sociological Methods & Research*, *36*(3), 297–326. https://doi.org/10.1177/0049124106292360

Yuan, X., Chen, D., Li, C., Wang, L., & Wang, W. (2016). Arctic sea Ice seasonal prediction by a linear Markov model. *Journal of Climate*, *29*(22), 8151–8173. https://doi.org/10.1175/JCLI-D-15-0858.1

Yumashev, D., van Hussen, K., Gille, J., & Whiteman, G. (2017). Towards a balanced view of Arctic shipping: Estimating economic impacts of emissions from increased traffic on the Northern Sea route. *Climatic Change*, *143*(1), 143–155. https://doi.org/10.1007/s10584-017-1980-6

Zhang, J., Steele, M., Lindsay, R., Schweiger, A., & Morison, J. (2008). Ensemble 1-year predictions of Arctic sea ice for the spring and summer of 2008. *Geophysical Research Letters*, *35*(8). https://doi.org/10.1029/2008GL033244

Zhu, S., Fu, X., Ng, A. K. Y., Luo, M., & Ge, Y.-E. (2018). The environmental costs and economic implications of container shipping on the Northern Sea route. *Maritime Policy & Management*, *45*(4), 456–477. https://doi.org/10.1080/03088839.2018.1443228

Zuur, A., Ieno, E. N., Walker, N., Saveliev, A. A., & Smith, G. M. (2009). *Mixed effects models and extensions in ecology with R*. Springer-Verlag. https://doi.org/10.1007/978-0-387-87458-6.